Analysis of Breakdown Characteristics of Field-Plate AlGaN/GaN HEMTs with a High-*k* Passivation Layer

T. Kabemura, H. Hanawa, and K. Horio

Faculty of Systems Engineering, Shibaura Institute of Technology
307 Fukasaku, Minuma-ku, Saitama 337-8570, Japan, horio@sic.shibaura-it.ac.jp

ABSTRACT

It is well known that the introduction of field plate increases the breakdown voltage V_{br} of AlGaN/GaN HEMTs. As another way to improve V_{br}, using a high-*k* passivation layer is proposed. So, in this study, we combine the two factors and analyzed the breakdown characteristics of field-plate AlGaN/GaN HEMTs as parameters of its rength L_{FP} and the relative permittivity of passivation layer ε_{r}. It is shown that the enhancement of V_{br} with increasing ε_{r} is more significant when L_{FP} is relatively short. There is an optimum value of L_{FP} to obtain the highest V_{br}, and it is around 0.2 and 0.3 μm when the gate-to-drain distance is 1.5 μm. When L_{FP} = 0.3 μm and ε_{r} takes a high value of 50, the electric field between the field-plate edge and the drain becomes rather uniform, and V_{br} becomes about 400 V, which corresponds to an effective electric field of 2.7 MV/cm between gate and drain.

Keywords: GaN HEMT, breakdown voltage, field plate, high-*k* passivation layer

1 INTRODUCTION

AlGaN/GaN HEMTs are now attractive for applications to high-power microwave devices and high-power switching devices [1, 2]. It is well known that introducing a field plate improves the power performance of AlGaN/GaN HEMTs as well as GaAs-based devices [3-5]. This is because the field plate reduce current collapse [6, 7], and also increase the breakdown voltage V_{br} [8-10].

To increase V_{br}, the introduction of passivation layer with high permittivity (high-*k* layer) is also considered [11-13]. In a previous work [12, 13], we analyzed off-state breakdown characteristics in AlGaN/GaN HEMTs as a parameter of relative permittivity of passivation layer ε_{r}, and found that V_{br} increased as ε_{r} increased.

Therefore, in this study, we combine the two structures and analyzed the breakdown characteristics of field-plate AlGaN/GaN HEMTs with a high-*k* passivation layer, and investigate how V_{br} is enhanced.

2 PHYSICAL MODEL

Fig.1 shows a device structure analyzed in this study. The gate length L_{G} is 0.3 μm and the gate-to-drain distance L_{GD} is 1.5 μm. The thickness of passivation layer d is 0.1 μm. The field-plate length L_{FP} is varied between 0 and 1 μm. The relative permittivity of the passivation layer ε_{r} is varied between 1 and 50. In a semi-insulating buffer layer, we consider a shallow donor, a deep donor, and a deep acceptor [14-16]. As an energy level of the deep acceptor, we consider E_{C} – 2.85 eV (E_{V} + 0.6 eV). For impurity compensation, we consider E_{C} – 0.5 eV as an energy level of the deep donor. The deep-acceptor density N_{DA} is set rather high of 10^{17} cm^{-3}.

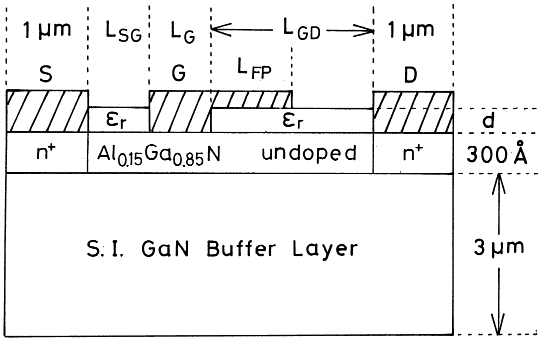

Figure 1: Device structure analyzed in this study.

Basic equations to be solved are Poisson's equation including ionized deep-level terms and continuity equations for electrons and holes including a carrier generation rate by impact ionization and carrier loss rates via the deep levels [13, 17-19]. These equations are expressed as follows.

1) Poisson's equation

$$\nabla \bullet (\varepsilon \nabla \psi) = -q(p - n + N_{\mathrm{Di}} + N_{\mathrm{DD}}^{+} - N_{\mathrm{DA}}^{-}) \qquad (1)$$

2) Continuity equations for electrons and holes

$$\nabla \bullet J_n = -qG + q(R_{\mathrm{DD}} + R_{\mathrm{DA}}) \qquad (2)$$

$$\nabla \bullet J_p = qG - q(R_{\mathrm{DD}} + R_{\mathrm{DA}}) \qquad (3)$$

where N_{DD}^{+} and N_{DA}^{-} are the ionized deep-donor and deep-acceptor densities, respectively. R_{DD} and R_{DA} represent carrier recombination rates via the deep donors and the deep acceptors, respectively. G is a carrier generation rate by impact ionization, and given by

$$G = (\alpha_n \,|\, J_n \,| + \alpha_p \,|\, J_p \,|) / q \qquad (4)$$

where α_n and α_p are ionization rates for electrons and holes, respectively, and expressed as

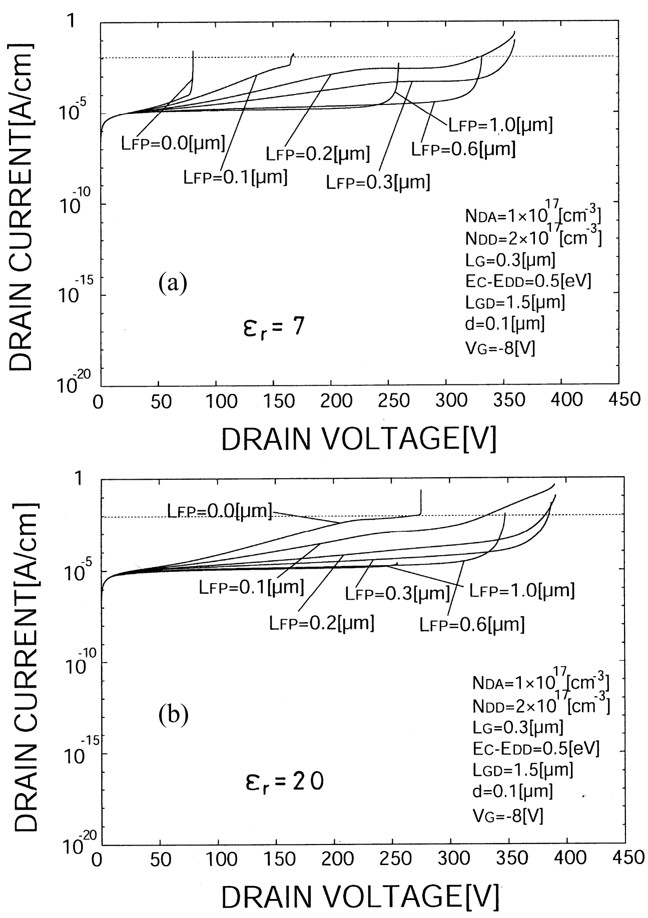

Figure 2: Calculated I_D-V_D curves as a parameter of L_{FP}. (a) $\varepsilon_r = 7$, (b) $\varepsilon_r = 20$. The dotted lines show 1 mA/mm.

$$\alpha_n = A_n \exp(-B_n / | E |) \tag{5}$$

$$\alpha_p = A_p \exp(-B_p / | E |) \tag{6}$$

where E is the electric field. A_n, B_n, A_p, and B_p are deduced from [20]. The above basic equations are put into discrete forms and solved numerically.

3 RESULTS AND DISCUSSIONS

Figs.2(a) and (b) show a comparison of calculated drain current I_D – drain voltage V_D curves of AlGaN/GaN HEMTs as a parameter of L_{FP} between the two cases with $\varepsilon_r = 7$ (SiN) and 20, respectively. The gate voltage is – 8 V, which corresponds to an off state. In both cases, the drain current usually increases suddenly, showing breakdown (except for $\varepsilon_r = 20$ and $L_{FP} = 0.1$ μm). This is due to impact ionization of carriers. Overall, the breakdown voltage seems to be higher in the case of $\varepsilon_r = 20$. Particularly, it is higher at relatively short L_{FP}.

Fig.3 shows a comparison of electric field profiles at the heterojunction interface for $L_{FP} = 0$ between the two cases with $\varepsilon_r = 7$ and 20. In the case of $\varepsilon_r = 7$, the increase in the drain voltage is entirely applied along the drain edge of the gate, leading to the breakdown at about 80 V. On the other hand, in the case of $\varepsilon_r = 20$, the electric field at the drain edge of the gate is reduced, and the high field region extends to the drain. Hence, the breakdown voltage increases to about 250 V. Here the breakdown voltage is defined as a drain voltage where the drain current becomes 1 mA/mm.

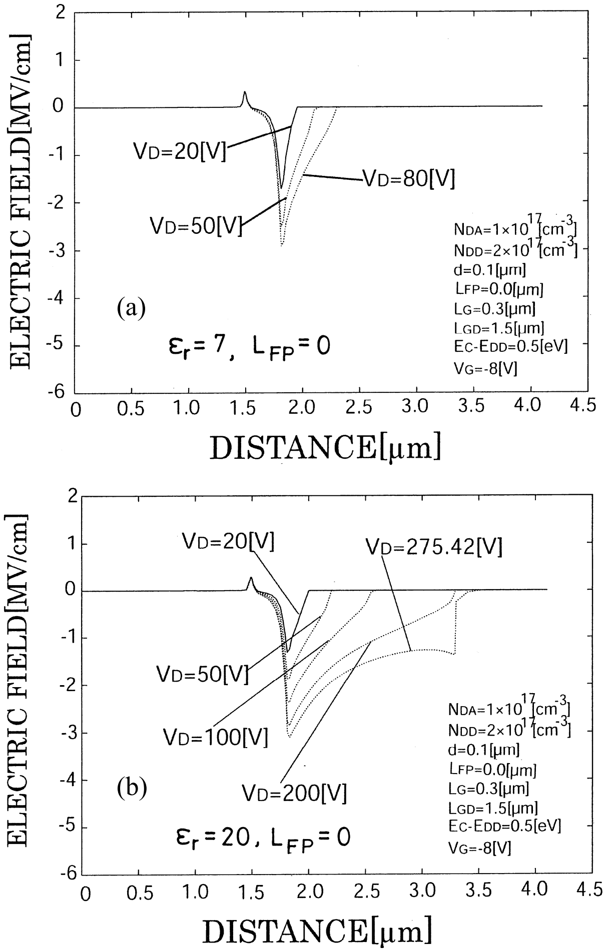

Figure 3: Electric field profiles along the heterojunction interface. $L_{FP} = 0$. (a) $\varepsilon_r = 7$, (b) $\varepsilon_r = 20$.

Fig.4 shows a comparison of electric field profiles at the heterojunction interface for $L_{FP} = 0.1$ μm between the two cases with $\varepsilon_r = 7$ and 20. In the case of $\varepsilon_r = 7$, the reduction of electric field at the drain edge is not so significant, leading to the abrupt increase in the drain current at $V_D = 168$ V. On the other hand, in the case of $\varepsilon_r = 20$, the electric field at the drain edge of gate is greatly reduced, and the electric field between the gate and drain remains around 3 MV/cm at $V_D = 390$ V, which is the breakdown voltage. In this case, as shown in Fig.2(b), the drain current does not show an abrupt increase, but increase gradually to reach 1 mA/mm. Here, the buffer leakage current determines the breakdown voltage.

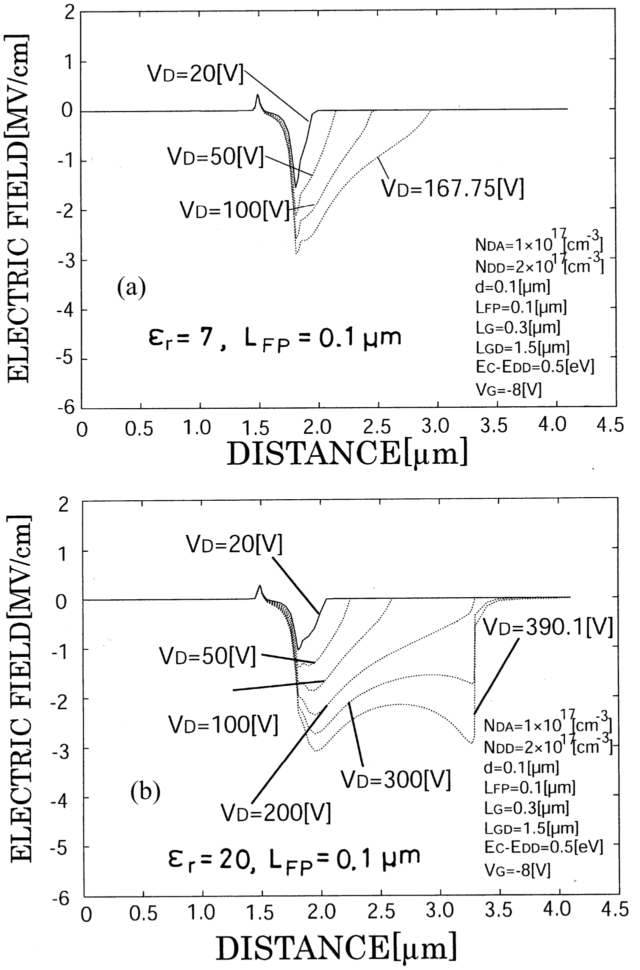

Figure 4: Electric field profiles along the heterojunction interface. L_{FP} = 0.1 μm.. (a) $\varepsilon_r = 7$, (b) $\varepsilon_r = 20$.

Fig.5 shows the breakdown voltage V_{br} as a function of the field-plate length L_{FP}, with ε_r as a parameter. It is seen that V_{br} is higher when ε_r is higher, particularly in the region where L_{FP} is relatively short. V_{br} becomes low when L_{FP} becomes relatively long. This is because the distance between the field-plate edge and the drain becomes short and the electric field in this region becomes very high. Hence, there is an optimum field-plate length to obtain high V_{br}, and it is around 0.2 and 0.3 μm here.

Fig.6 shows a comparison of electric field profiles at L_{FP} = 0.3 μm between the two cases with $\varepsilon_r = 7$ and 50. In both cases, electric field at the drain edge of the gate is reduced, and the breakdown voltage is determined by the electric field between the field-plate edge and the drain. In the case of $\varepsilon_r = 50$, the electric field in this region is more uniform. This is due to the high-*k* dielectric, and hence V_{br} becomes higher (about 400 V) than that for lower ε_r.

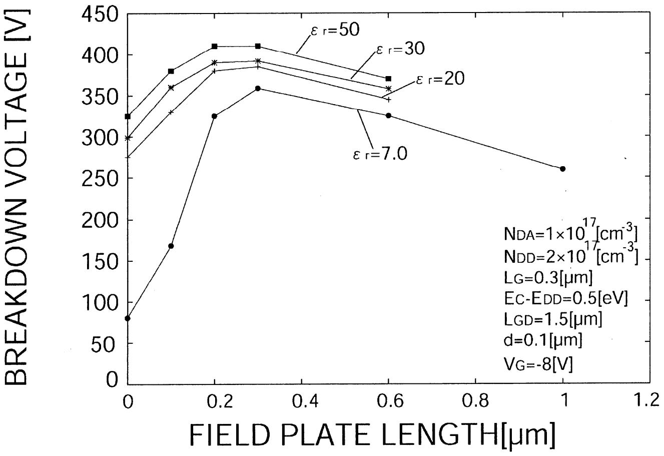

Figure 5: Breakdown voltage V_{br} versus field-plate length L_{FP} curves, with ε_r as a parameter.

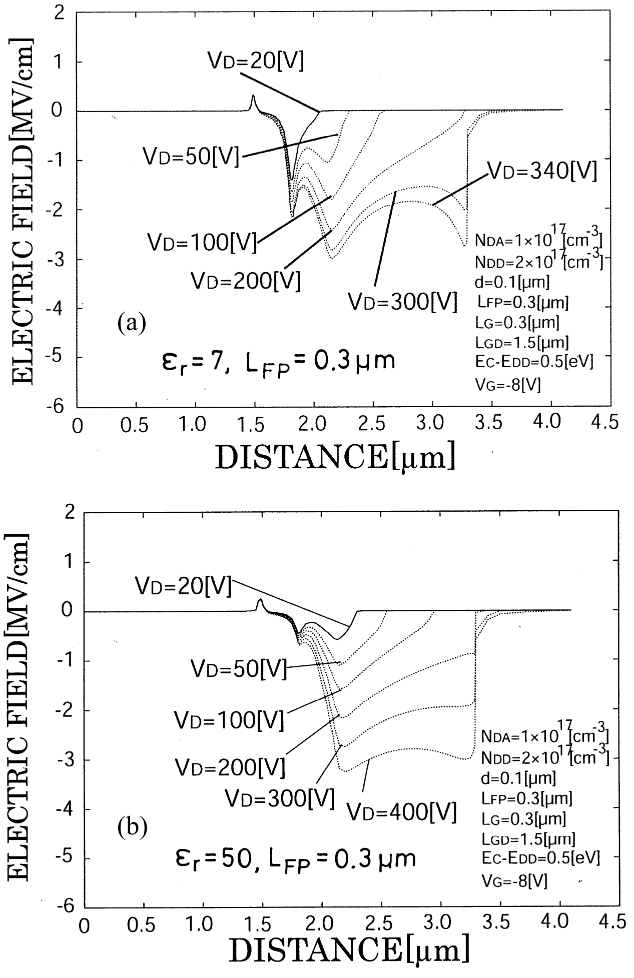

Figure 6: Electric field profiles along the heterojunction interface. L_{FP} = 0.3 μm.. (a) $\varepsilon_r = 7$, (b) $\varepsilon_r = 50$.

4 CONCLUSION

In summary, we have performed a two-dimensional analysis of breakdown characteristics of field-plate AlGaN/GaN HEMTs as parameters of its rength L_{FP} and the relative permittivity of passivation layer ε_r. It has been shown that V_{br} is higher when ε_r becomes higher, particularly in the region where L_{FP} is short. This is because the electric field at the drain edge of gate is effectively reduced even for short L_{FP}. It has also been shown that there is an optimum value of L_{FP} to obtain highest V_{br}, and it is around 0.2 and 0.3 μm when the gate-to-drain distance is 1.5 μm. When ε_r has a high value of 50, the electric field between the field-plate edge and the drain becomes rather uniform, and V_{br} reachess about 400 V, which corresponds to an effective electric field of 2.7 MV/cm between the gate and the drain.

REFERENCES

[1] U. K. Mishra, L. Shen, T. E. Kazior, and Y.-F. Wu, "GaN-based RF power devices and amplifiers", Proc. IEEE, vol.96, pp.287-305, 2008.

[2] N. Ikeda, Y. Niiyama, H. Kambayashi, Y. Sato, T. Nomura, S. Kato, and S. Yoshida, "GaN power transistors on Si substrates for switching applications", Proc. IEEE, vol.98, pp.1151-1161, 2010.

[3] A. Wakejima, K. Ota, K. Matsunaga, and M. Kuzuhara, "A GaAs-based field-modulating plate HFET with improved WCDMA peak-output-power characteristics", IEEE Trans. Electron Devices, vol.50, pp.1983-1987, Sep. 2003

[4] Y.-F. Wu, A. Saxler, M. Moore, R. P. Smith, S. Sheppard, P. M. Chavarkar, T. Wisleder, U. K. Mishra, and P. Parikh, "30-W/mm GaN HEMTs by field plate optimization", IEEE Electron Device Lett., vol.25, pp.117-119, 2004.

[5] Y. Hao, L. Yang, X. Ma, J. Ma, M. Cao, C. Pan, C. Wang, and I. Zhang, "High-performance microwave gate-recessed AlGaN/AlN/GaN MOS-HEMT with 73% power-added efficiency", IEEE Electron Device Lett., vol.32, pp.626-628, 2011.

[6] K. Horio, A. Nakajima, and K. Itagaki, "Analysis of field-plate effects on buffer-related lag phenomena and current collapse in GaN MESFETs and AlGaN/GaN HEMTs", Semicond. Sci. Technol., vol.24, pp.085022-1–085022-7, 2009.

[7] K. Horio, T. Tanaka, K. Itagaki and A. Nakajima, "Two-dimensional analysis of field-plate effects on surface state-related current transients and power slump in GaAs FETs", IEEE Trans. Electron Devices, vol.58, pp. 698-703, 2011.

[8] S. Karmalkar and U. K. Mishra, "Enhancement of breakdown voltage in AlGaN/GaN high electron mobility transistors using a field plate", IEEE Trans. Electron Devices, vol.48, pp.1515-1521, 2001.

[9] E. Bahat-Treidel, O. Hilt, F. Brunner, V. Sidorov, J. Würfl, and G. Tränkle, "AlGaN/GaN/AlGaN DH-HEMTs breakdown voltage enhancement using multiple gating field plates (MGFPs)", IEEE Trans. Electron Devices, vol.57, pp.1208-1216, 2010.

[10] H. Onodera and K. Horio, "Analysis of buffer-impurity and field-plate effects on breakdown characteristics in small sized AlGaN/GaN high electron mobility transistors", Semicond. Sci. Technol., vol.27, pp.085016-1–085016-6, 2012.

[11] Q. Luo and Q. Yu, "Electric field modulation by introducing a *HK* dielectric film of tens of nanometers in AlGaN/GaN HEMT", Nanosci. Nanotechnol. Lett., vol.4, pp.936-939, 2012.

[12] H. Hanawa and K. Horio, "Increase in breakdown voltage of AlGaN/GaN HEMTs with a high-*k* dielectric layer", Phys. Status Solidi A, vol.211, pp.784-787, 2014.

[13] H. Hanawa, H. Onodera, A. Nakajima, and K. Horio, "Numerical analysis of breakdown voltage enhancement in AlGaN/GaN HEMTs with a high-*k* passivation layer", IEEE Trans. Electron Devices, vol.61, pp.769-775, 2014.

[14] K. Horio, K. Yonemoto, H. Takayanagi, and H. Nakano, "Physics-based simulation of buffer-trapping effects on slow current transients and current collapse in GaN field effect transistors", J. Appl. Phys., vol.98, pp.124502-1–124502-7, 2005.

[15] K. Horio and A. Nakajima, "Physical mechanism of buffer-related current transients and current slump in AlGaN/GaN high electron mobility transistors", Jpn. J. Appl. Phys., vol.47, pp.3428-3433, 2008.

[16] K. Horio, H. Onodera, and A. Nakajima, "Analysis of backside-electrode and gate-field-plate effects on buffer-related current collapse in AlGaN/GaN high electron mobility transistors", J. Appl. Phys., vol.109, pp.114508-1–114508-7, 2011.

[17] K. Horio and A. Wakabayashi, "Numerical analysis of surface-state effects on kink phenomena of GaAs MESFETs", IEEE Trans. Electron Devices, vol.47, pp.2270-2276, 2000.

[18] Y. Mitani, D. Kasai and K. Horio, "Analysis of surface-state and impact-ionization effects on breakdown characteristics and gate-lag phenomena in narrowly-recessed-gate GaAs FETs", IEEE Trans. Electron Devices, vol.50, pp.285-291, 2003.

[19] Y. Kazami, D. Kasai and K. Horio, "Numerical analysis of slow current transients and power compression in GaAs FETs", IEEE Trans. Electron Devices, vol.51, pp.1760-1764, 2004.

[20] C. Bulutay, "Electron initiated impact ionization in AlGaN alloys", Semicond. Sci. Technol., vol.17, pp.59-62, 2002.